

**Paper-based Fluorogenic RNA Aptamer Sensors for Label-Free Detection of Small Molecules**

|                               |  |
|-------------------------------|--|
| Journal:                      | <i>Analytical Methods</i>  |
| Manuscript ID                 | AY-ART-03-2020-000588.R1   |
| Article Type:                 | Paper  |
| Date Submitted by the Author: | 02-May-2020  |
| Complete List of Authors:     | Shafiei, Fatemeh; University of Massachusetts Amherst, Chemistry<br>McAuliffe, Kathleen; University of Massachusetts Amherst, Chemistry<br>Bagheri, Yousef; University of Massachusetts Amherst, Chemistry;<br>University of Massachusetts amherst<br>Sun, Zhining; University of Massachusetts Amherst, Chemistry<br>Yu, Qikun; UMass Amherst, Chemistry<br>Wu, Rigumula; UMass Amherst, Chemistry<br>You, Mingxu; UMass Amherst, Chemistry |
|                               |  |

# Paper-based Fluorogenic RNA Aptamer Sensors for Label-Free Detection of Small Molecules

Fatemeh Shafiei,<sup>a</sup> Kathleen McAuliffe,<sup>a</sup> Yousef Bagheri,<sup>a</sup> Zhining Sun,<sup>a</sup> Qikun Yu,<sup>a</sup> Rigumula Wu,<sup>\*a</sup> and Mingxu You<sup>\*a</sup>

<sup>a</sup> Department of Chemistry, University of Massachusetts, Amherst, Massachusetts 01003, USA

\* Correspondence authors

E-mail: [rigumulawu@umass.edu](mailto:rigumulawu@umass.edu); [mingxuyou@umass.edu](mailto:mingxuyou@umass.edu)

## Abstract

Sensors based on fluorogenic RNA aptamers have emerged in recent years. These sensors have been used for *in vitro* and intracellular detection of a broad range of biological and medical targets. However, the potential application of fluorogenic RNA-based sensors for point-of-care testing is still little studied. Here, we report a paper substrate-based portable fluorogenic RNA sensor system. Target detection can be simply performed by rehydration of RNA sensor-embedded filter papers. This affordable sensor system can be used for the selective, sensitive, and rapid detection of different target analytes, such as antibiotics and cellular signaling molecules. We believe these paper-based fluorogenic RNA sensors exhibit a great potential for point-of-care testing of a wide range of target from small molecules, nucleic acids, proteins, to various pathogens.

## Introduction

There are growing numbers of diseases and health threats all around the world. Issues with environmental contamination and food qualities also keep increasing. Accurate, easy-to-use, and affordable point-of-care testing is highly desired<sup>1-4</sup>. A large number of point-of-care devices have been developed for various applications ranging from glucose testing, pregnancy testing, food pathogen detection, to disease diagnostics<sup>5-8</sup>. Ideal point-of-care techniques should exhibit high sensitivity and specificity, eliminating the need for lengthy tests or expensive laboratory equipment, and easy to be operated by people without special training<sup>9,10</sup>.

Among different probes used in point-of-care devices, nucleic acids, especially DNA aptamers, are promising candidates for the detection of various target analytes<sup>6,11-13</sup>. Aptamers are single-stranded DNAs or RNAs that exhibit high affinity and specificity towards their targets. For a given target, aptamers can be identified through a systematic evolution of ligands by exponential enrichment (SELEX) process<sup>14,15</sup>. As a result, aptamer-based sensors can be facilely engineered for a large variety of target analytes. However, the broad applications of DNA aptamer-based point-of-care devices are still limited. This is partially because of their reduced target-specificity in the complex biological samples and the high cost of synthesizing dye/indicator-modified strands<sup>16,17</sup>.

In recent years, a type of fluorogenic RNA aptamer, such as so-called Spinach or Broccoli, have become popular in developing biosensors<sup>18-21</sup>. Spinach/Broccoli can label-free bind and activate the fluorescence of dyes such as 3,5-difluoro-4-hydroxybenzylidene-1-trifluoroethyl-imidazolinone (DFHBI-1T). We and others have engineered Spinach/Broccoli into sensors for both in vitro and live-cell detection of metabolites, ions, proteins, and RNAs<sup>18,22-29</sup>. In these sensors, the target-binding RNA aptamer domain is highly selective, even in complex cellular environment. The targeting-binding property of many of these RNA aptamers (or riboswitches) have been developed and tested through natural evolution. In addition, these fluorogenic RNA sensors can be incorporated with various genetic circuits to further improve the sensitivity and performance of the device<sup>23,27</sup>. As a result, we believe these fluorogenic RNA aptamer-based sensors can be potentially useful in developing point-of-care devices with high selectivity and sensitivity.

Most of existing fluorogenic RNA-based in vitro detection are performed in a sample solution using a cuvette setting. However, this setup is not user-friendly for

1  
2  
3 point-of-care testing. In this study, we asked if these fluorogenic RNA sensors can be  
4 applied in portable devices, such as paper substrates. Naturally existing cellulose-  
5 based material, such as papers, are popularly used substrates for point-of-care  
6 testing<sup>3,10,13</sup>. Papers are compatible with biological samples and can be chemically  
7 modified to incorporate different functional groups. The intrinsic porous structure of  
8 papers allow the storage of probes in the cellulose matrix. In addition, white-  
9 background papers are good candidates for colorimetric or fluorometric tests with  
10 minimal interference in the resultant optical signal.  
11  
12  
13  
14

15 Here, for the first time, we report the development of paper-based fluorogenic  
16 RNA aptamer devices for potential point-of-care applications. As a proof of concept, we  
17 demonstrated that these RNA-based portable devices can be used for the sensitive,  
18 selective, and accurate detection of antibiotics and signaling molecules. These paper-  
19 based devices can be stored for several months at room temperature without affecting  
20 the sensor behavior. Detection is simply performed by adding drops of target sample  
21 onto sensor-embedded filter papers. The resulting signal can be detected within 15–30  
22 min. We believe these paper-based fluorogenic RNA aptamer devices can be  
23 potentially useful for point-of-care testing of various biological, medical, and daily life  
24 targets.  
25  
26  
27  
28  
29  
30

## 31 **Materials and Methods**

32  
33

34 **Chemicals and reagents.** All the chemicals and reagents were purchased from Sigma  
35 or Fisher unless otherwise stated and used without further purification. Guanosine  
36 tetraphosphate was purchased from Jena Bioscience (Germany). DNA oligonucleotides  
37 were synthesized and purified by Integrated DNA Technologies, Inc. or Keck Oligo  
38 Synthesis Lab at Yale University. The stock DNA oligonucleotides were dissolved at  
39 100  $\mu$ M concentration in 10 mM Tris-HCl, 0.1 mM EDTA at pH= 7.5 and stored at -20°C.  
40 Double-stranded DNA template/non-template duplexes for *in vitro* RNA transcription  
41 were prepared by PCR amplification using an Eppendorf Mastercycler. The PCR  
42 product was further purified using a QIAquick PCR purification kit (Qiagen,  
43 Germantown, MD). The concentrations of nucleic acids were measured using a  
44 NanoDrop One UV-Vis spectrophotometer. All the RNAs for *in vitro* test were  
45 transcribed using a HiScribe™ T7 high yield RNA synthesis kit (New England BioLabs,  
46 Ipswich, MA), and then treated with RNase-free DNase I (New England BioLabs) and  
47 further purified by a Sephadex G-25 column (GE Life Sciences). The final RNA product  
48 was verified by running 10% denaturing PAGE gels. These RNA strands were prepared  
49 into aliquots and stored at -20°C for immediate usage or at -80°C for long-term storage.  
50 All the RNA structures were designed using the NUPACK and Mfold online software.  
51  
52  
53  
54  
55  
56  
57  
58  
59  
60

1  
2  
3  
4 **Solution-phase fluorescence assay.** All the solution-based fluorescence  
5 measurements were conducted with a PTI fluorimeter (Horiba, New Jersey, NJ).  
6 Fluorescence assay and the assembly of RNA strands were conducted in a buffer  
7 consisting of 10 mM Tris, 5 mM MgCl<sub>2</sub>, and 100 mM KCl at pH 7.5. In our  
8 measurement, fluorescence spectra in the range of 500–550 nm were collected by  
9 exciting at 480 nm.  
10  
11  
12

13  
14 **Preparation of RNA-incorporated filter papers.** Paper disks were prepared by  
15 cutting fine grade filter paper (Whatman ashless filter paper, Grade 42, 2.5 μm nominal  
16 particle retention, #1442-042) with hole punchers of different diameters. The paper  
17 disks were then autoclaved and treated with bovine serum albumin (BSA). RNA probes  
18 were mixed in folding buffer consisting of 40 mM HEPES, 100 mM KCl, 0.1% DMSO  
19 and 1 mM MgCl<sub>2</sub>, at pH 7.5 and then loaded to the prepared paper disks. Afterwards,  
20 RNA-incorporated paper disks were flash frozen in liquid nitrogen and then dried out in  
21 a lyophilizer.  
22  
23  
24

25  
26 **Paper-based target detection and data analysis.** To detect target concentration, 8  
27 μL of sample solution was directly added onto the above-prepared RNA-incorporated  
28 paper disks. In-paper fluorescence detection was performed with a Typhoon™ FLA  
29 9500 biomolecular imager (GE Life Sciences). A 480 nm laser was used for excitation  
30 and emission signal was collected at ~520 nm. While for potential point-of-care testing,  
31 a portable UV lamp could be an option. All the data analysis was performed using an  
32 ImageJ software and data plotting and fitting were accomplished by the Origin software.  
33  
34  
35

36 **Preparation of cell lysate.** Cell lysate preparation was performed following the  
37 previously reported method<sup>30</sup>. Briefly, 10 mL of overnight grown *E. coli* cells were  
38 treated with 1 mL of 1.9% formaldehyde solution and then incubated at 4°C for 20 min.  
39 Cells were then precipitated by centrifugation and the supernatant was removed.  
40 Afterwards, cell pellets were resuspended in 0.5 mL of 0.1 mM KOH solution at 4°C for  
41 30 min. The obtained solution was neutralized by H<sub>3</sub>PO<sub>4</sub> and cell debris were then  
42 separated by centrifugation. Cell lysate was finally directly added onto RNA-  
43 incorporated paper disks for the target detection.  
44  
45  
46  
47  
48

## 49 **Results and Discussion**

### 50 **Performance of Broccoli in the paper disks**

51  
52 First, we asked if fluorogenic RNAs, e.g., Broccoli, could still function effectively and  
53 activate the fluorescence of DFHBI-1T in the paper substrate. Here we chose to use a  
54  
55  
56  
57  
58  
59  
60

1  
2  
3 fine grade Whatman® ashless filter paper, which contains >98% of highly stable and  
4 polymerized  $\alpha$ -cellulose. We expect that RNA probes can be potentially stored within  
5 these filter papers. Indeed, the function of synthetic RNA-mediated gene network has  
6 been demonstrated in this type of paper<sup>13</sup>.  
7  
8  
9

10 We chose to use Broccoli, a 49-nucleotide-long aptamer (Table S1) that exhibits  
11 bright green fluorescence upon binding with DFHBI-1T<sup>18</sup>. We added 20  $\mu$ M DFHBI-1T  
12 (0.16 nmol) into the filter papers (5 mm in diameter), in the presence or absence of 1  
13  $\mu$ M Broccoli (8 pmol), and then freeze-dried overnight. Afterwards, the papers were  
14 rehydrated with nuclease-free water and the fluorescence signal was detected after 30  
15 min incubation. Indeed, a 3.1-fold increase in the fluorescence intensity was observed  
16 in the presence of Broccoli (Fig. 1a). Broccoli RNA can still fold and bind with DFHBI-  
17 1T within paper substrate.  
18  
19  
20  
21

22 Next, we asked if we could optimize the fluorescence intensity of Broccoli/DFHBI-  
23 1T complex in the filter papers. It is known that bovine serum albumin (BSA), a  
24 commonly used blocking reagent, could be used to reduce the non-specific interactions  
25 between cellulose matrix and nucleic acids<sup>31,32</sup>. We wondered if the addition of BSA will  
26 affect the folding of Broccoli and/or its binding with DFHBI-1T. To test this, we  
27 pretreated filter papers with buffers containing different percentage of BSA and then  
28 added Broccoli/DFHBI-1T complex (Fig. 1a). Indeed, by treating with BSA, the  
29 fluorescence signal of Broccoli can be improved in the filter papers. Our result shows  
30 that 0.75% BSA-pretreated papers exhibited the largest fold of fluorescence  
31 enhancement (5.0-fold). For the following experiments, the filter papers were all  
32 pretreated with 0.75% BSA.  
33  
34  
35  
36  
37

38 A fast response kinetics is desirable for a point-of-care device. To study the  
39 fluorescence activation kinetics of Broccoli in this paper substrate, we monitored the  
40 change of fluorescence signal immediately after mixing 1  $\mu$ M Broccoli (8 pmol) with 20  
41  $\mu$ M DFHBI-1T (0.16 nmol) in the paper disks. A fast increase in the fluorescence signal  
42 was observed (Figure 1b). It took  $\sim$ 9 min to reach half-maximal fluorescence signal,  
43 and  $\sim$ 24 min to reach 90% of the maximal signal. Indeed, the fluorescence signal of  
44 Broccoli can be quickly activated in the paper substrate.  
45  
46  
47

48 We next wanted to study the correlation between the Broccoli concentration and  
49 fluorescence intensity in the paper substrate. For this purpose, 0.01–10  $\mu$ M of Broccoli  
50 RNA (0.08–80 pmol) was incubated with 20  $\mu$ M DFHBI-1T and the corresponding  
51 fluorescence was determined. A nice sigmoid correlation was observed between the  
52 RNA concentration and the fluorescence intensity (Fig. 1c). If we defined the dynamic  
53 range as that induced 10%–90% of maximum fluorescence, a moderate dynamic range  
54  
55  
56  
57  
58  
59  
60

1  
2  
3 was observed with 0.3–5  $\mu\text{M}$  of RNA. We also compared the fluorescence signal in the  
4 papers before and after the freeze-drying process. A quite similar fluorescence  
5 response was observed even after 48 h of lyophilization (Fig. 1c). Freeze-drying  
6 process did not affect the performance of Broccoli. Broccoli fluorescence signal can be  
7 directly correlated with the RNA concentrations in the paper.  
8  
9

10  
11 We have further determined the detection limit of this paper-based system. Our  
12 results indicated that as low as 0.2  $\mu\text{M}$  (1.6 pmol) Broccoli can be detected in the paper  
13 substrate when 20  $\mu\text{M}$  DFHBI-1T was used (Fig. 1c). For the smallest size of paper  
14 disk (1.6 mm in diameter) we used, with only 0.5  $\mu\text{L}$  of sample was needed, as low as  
15 0.1 picomole Broccoli RNA can be reliably detected (Fig. S1). Indeed, these paper-  
16 based devices are highly sensitive and can be used for detecting small amount of  
17 fluorogenic RNAs.  
18  
19  
20  
21

22 It is also important for a point-of-care device to be stable for a long period of time  
23 under normal storage condition. To test the stability of fluorogenic RNAs in the paper  
24 substrate, we first embedded 1  $\mu\text{M}$  Broccoli and 20  $\mu\text{M}$  DFHBI-1T into 0.75% BSA-  
25 coated papers and freeze-dried. After stored at room temperature for different periods  
26 of time, the fluorescence signal in the paper was measured after rehydration. Broccoli  
27 was quite stable in the paper, >50% fluorescence signal was conserved after one week  
28 storage, ~30% fluorescence still exhibited even after >200 days storage at room  
29 temperature (Fig. 1d). We think the RNA degradation should be the major reason for  
30 the observed fluorescence decay. By adding RNase inhibitors and pretreating the  
31 paper substrate and container, the RNA degradation could be potentially further  
32 reduced.  
33  
34  
35  
36  
37

38 Taken together, our results showed that Broccoli can effectively fold in the paper  
39 substrates and activate the fluorescence signal of DFHBI-1T. These fluorogenic RNA  
40 aptamers can be potentially used to develop sensors for point-of-care testing.  
41  
42

### 43 **Paper-based Broccoli sensors for the detection of antibiotics**

44 After optimizing the performance of Broccoli in the paper, we next asked if Broccoli  
45 RNA-based sensors could also function in the paper substrates. For this purpose, we  
46 first selected tetracycline as a target molecule. Tetracycline is one widely used type of  
47 antibiotics for the treatment of bacterial infections<sup>33</sup>. The existence and leftover of  
48 tetracycline in drinking water, agricultural and dairy products has been shown to induce  
49 bacterial antibiotic resistance<sup>34</sup>. It is thus important to develop point-of-care devices to  
50 rapidly detect tetracycline in these real life samples.  
51  
52  
53  
54  
55  
56  
57  
58  
59  
60

1  
2  
3 We and others have recently engineered a type of allosteric sensor based on  
4 fluorogenic RNA aptamers<sup>18–29</sup>. By fusing a target-binding aptamer with fluorogenic  
5 RNA, sensors can be developed for different analytes, including tetracycline<sup>26,28</sup>. Here,  
6 we engineered a Broccoli-based tetracycline sensor (Table S1) and then applied it for  
7 the detection of tetracycline in the paper substrate. In our sensor design, the binding of  
8 tetracycline with the aptamer region induced the folding of Broccoli, which will further  
9 activate the fluorescence of DFHBI-1T and give bright green fluorescence (Fig. 2a). An  
10 F30 three-way junction RNA scaffold was further used to improve the folding and  
11 stability of the whole sensor.  
12  
13  
14  
15

16 To test the performance of this tetracycline sensor in the paper, 1  $\mu\text{M}$  in vitro  
17 transcribed sensor RNA and 10  $\mu\text{M}$  DFHBI-1T was embedded into the filter paper and  
18 freeze-dried overnight. After rehydration and incubation for 30 min, indeed, a 1.7-fold,  
19 3.6-fold, and 4.3-fold increase in the fluorescence signal was observed in the presence  
20 of 100, 750, and 1000  $\mu\text{M}$  of tetracycline. To further study the tetracycline concentration  
21 range that these sensors could detect, a dose-response curve was generated (Fig. 2b).  
22 Under our experimental condition, the half-maximal fluorescence was reached after  
23 adding  $\sim 250$   $\mu\text{M}$  tetracycline. A moderate dynamic range of tetracycline, 0.1–0.8 mM  
24 (0.8–6.4 nmol), can induce 10%–90% of maximum fluorescence. Indeed, these paper-  
25 based tetracycline sensors can be potentially suitable for the detection of tetracycline in  
26 real samples<sup>34</sup>.  
27  
28  
29  
30  
31

32 We next asked if these Broccoli-based tetracycline sensors could selectively  
33 recognize tetracycline over other antibiotics. We added 750  $\mu\text{M}$  of tetracycline,  
34 tobramycin, gentamicin, doxycycline, kanamycin, streptomycin, and ampicillin,  
35 respectively, into the sensor-embedded paper disks. As expected, the fluorescence  
36 signal was only activated in the presence of tetracycline (Fig. 3a). Indeed, these paper-  
37 based sensors can detect tetracycline with high selectivity.  
38  
39  
40

41 We further studied the fluorescence response kinetics of the tetracycline sensor.  
42 To investigate this, we start recording the fluorescence signal immediately after adding  
43 0.5, 0.75, and 1 mM of tetracycline (Fig. 2c). The fluorescence signal in the paper can  
44 be quickly observed. Half-maximal fluorescence and 90% of the maximal signal were  
45 reached around 15 min and 25 min, respectively.  
46  
47  
48

49 We also tested the stability of paper-based tetracycline sensors after a week-long  
50 storage at room temperature. As shown in Fig. 3b, the sensor can still be reliably used  
51 to detect tetracycline with only 23% loss in the fluorescence signal. Indeed, the freeze-  
52 dried RNA-embedded paper device is quite stable under normal storage condition.  
53  
54  
55  
56  
57  
58  
59  
60

1  
2  
3 All the previous tests were performed in RNase-free buffer, we next asked if  
4 these paper-based sensors can also function by adding real water sample. We started  
5 with local tap water (Amherst, MA, USA). After adding different amounts of tetracycline,  
6 indeed, the paper-based tetracycline sensor exhibited quite similar tetracycline-induced  
7 fluorescence intensity in both RNase-free water and tap water (Fig. S2).  
8  
9

10  
11 We next tested the performance of paper-based tetracycline sensors with surface  
12 water. For this purpose, we acquired water sample directly from the Connecticut River  
13 in the New England region of the United States. We then doped different  
14 concentrations of tetracycline into this river sample. After 30 min incubation in the  
15 paper embedded with 1  $\mu\text{M}$  RNA sensor and 10  $\mu\text{M}$  DFHBI-1T, the increase in the  
16 fluorescence signal (Fig. 2b) fitted nicely with the calibration curve determined in buffer.  
17 Broccoli-based sensors indeed can be used for tetracycline detection in the river  
18 sample. There was no detectable amount of tetracycline in the tested Connecticut River  
19 sample, but it could be interesting in the future to apply this paper device to detect  
20 tetracycline concentrations in other agricultural and dairy samples.  
21  
22  
23  
24

### 25 **Paper-based Broccoli sensors for the detection of signaling molecules**

26 We wondered if other Broccoli-based sensors could also function in the paper substrate.  
27 We chose guanosine tetraphosphate (ppGpp) as another example. PpGpp is an  
28 important signaling molecule that is produced in the bacterial cells for the stringent  
29 response<sup>30,35,36</sup>. The generation of ppGpp helps bacteria to survive under harsh  
30 condition by redistributing resources and regulating the expression of various enzymes  
31 and transcription factors<sup>36</sup>. It is critical to reliably and rapidly detect ppGpp in cell lysate  
32 and other biological samples. The standard methods for detecting ppGpp, such as  
33 liquid chromatography and thin layer chromatography<sup>35,36</sup>, are time consuming, normally  
34 require radioactive labeling, and can only be performed in some specialized  
35 laboratories. Here, we aimed to develop a paper-based sensor that is easy-to-use and  
36 able to detect ppGpp with high accuracy and selectivity.  
37  
38  
39  
40  
41  
42

43 We have recently engineered a Broccoli-based probe for detecting ppGpp in  
44 solution and in living cells (unpublished results). This probe is developed based on a  
45 highly selective ppGpp-targeting RNA aptamer that was naturally evolved to bind ppGpp  
46 with high affinity<sup>37,38</sup>. The binding of ppGpp to the aptamer induced the folding of  
47 Broccoli and activated the fluorescence of DFHBI-1T (Fig. 4a). After incorporating 1  $\mu\text{M}$   
48 RNA sensor and 10  $\mu\text{M}$  DFHBI-1T into the paper substrate and freeze-drying overnight,  
49 we added different concentrations of ppGpp. As expected, a 1.6–3.5-fold fluorescence  
50 enhancement was observed after adding 0.5–50  $\mu\text{M}$  ppGpp. A moderate concentration  
51 range, 0.1–10  $\mu\text{M}$ , of ppGpp (0.8–80 pmol) can be detected in this paper device (Fig.  
52  
53  
54  
55  
56  
57  
58  
59  
60

1  
2  
3 4b). After two-day storage at room temperature, a similar 0.1–20  $\mu\text{M}$  dynamic range  
4 was observed (Fig. 4d).  
5  
6

7 We also determined the sensor kinetics in the paper substrate. After adding 50  
8  $\mu\text{M}$  ppGpp, a fast fluorescence enhancement was observed, with half maximal  
9 fluorescence shown in  $\sim 7$  min and 90% of maximum signal in  $\sim 15$  min (Fig. 4c).  
10  
11

12 To test the selectivity of the sensor, the fluorescence intensity in the paper was  
13 measured adding 10  $\mu\text{M}$  ppGpp or several other analogs. As expected, the  
14 fluorescence signal of the sensor was not activated by ppGpp analogs, including PRPP,  
15 ATP, GTP, UTP, CTP and guanine (Fig. 5a). The paper-based sensor is quite selective  
16 towards ppGpp.  
17  
18

19  
20 Lastly, we asked if we can use this paper-based sensor to detect ppGpp in the  
21 cell lysate. To test the performance of sensors in the cell lysate, we first lysed 8  $\mu\text{L}$  of  
22 overnight grown *E. coli* cells and added different amounts of ppGpp. Based on the  
23 standard spike recovery test, 98% recovery was observed (Fig. 4b and 5b). Indeed, this  
24 paper-based sensor can be potentially used to detect ppGpp in real biological samples  
25 with minimum operation procedure.  
26  
27  
28  
29  
30

## 31 Conclusions

32  
33

34 We reported here the development of fluorogenic RNA-based sensors for detecting  
35 various targets in a piece of paper. We envision that these paper-based devices could  
36 have great potential for future point-of-care applications. Paper-based artificial genetic  
37 circuits have been recently developed for the selective and sensitive point-of-care  
38 detection of various targets, including small molecules, proteins, and pathogen  
39 RNAs<sup>11,13,31</sup>. Enzymes and fluorescent proteins are commonly used as reporters in  
40 these genetic network. Considering the complicated transcription and translation  
41 procedure of these circuits in generating signal readout, fluorogenic RNA-based  
42 sensors could potentially serve as an alternative or complementary reporting system.  
43 By conjugating some of existing genetic circuits with these fluorogenic RNAs, the  
44 sensitivity and kinetics of the system could be further improved.  
45  
46  
47  
48  
49

50 In this study, for the first time, fluorogenic RNA-based sensors were incorporated  
51 into the paper substrate for future *in situ* and label-free testing. These paper-based  
52 fluorogenic RNA sensors allow us to detect the target analytes in a cost-effective,  
53 selective, sensitive, and rapid pattern. These sensors can be easily operated by people  
54 without professional training. For future studies, we will test the possibility to use  
55  
56  
57  
58  
59  
60

1  
2  
3 handheld light sources to detect these RNA-mediated fluorescence signals in the paper.  
4 Considering aptamers can be easily generated for a largely variety of target analytes,  
5 we believe this novel fluorescent sensor platform can be used to develop affordable  
6 point-of-care devices for different ions, small molecules, proteins, RNAs, and  
7 pathogens.  
8  
9

## 10 11 12 13 14 **Acknowledgment**

15  
16 The authors gratefully acknowledge the UMass Amherst start-up grant, NIH  
17 R01AI136789, NSF CAREER, and Alfred P. Sloan Research Fellowship to M. You. The  
18 authors also thank other members in the You Lab for useful discussion and valuable  
19 comments.  
20  
21  
22  
23  
24  
25

## 26 27 **Conflict of Interests**

28  
29 The authors declare no conflict of interest.  
30  
31  
32  
33

## 34 35 **References**

- 36 1 R. W. Peeling and D. Mabey, *Clin. Microbiol. Infect.*, 2010, **16**, 1062–1069.
- 37 2 D. C. Christodouleas, B. Kaur and P. Chorti, *ACS Cent. Sci.*, 2018, **4**, 1600–1616.
- 38 3 A. St John and C. P. Price, *Clin. Biochem. Rev.*, 2014, **35**, 155–167.
- 39 4 P. K. Drain, E. P. Hyle, F. Noubary, K. A. Freedberg, D. Wilson, W. R. Bishai, W.  
40 Rodriguez and I. V Bassett, *Lancet. Infect. Dis.*, 2014, **14**, 239–249.
- 41 5 G. Xu, D. Nolder, J. Reboud, M. C. Oguike, D. A. van Schalkwyk, C. J. Sutherland  
42 and J. M. Cooper, *Angew. Chem. Int. Ed. Engl.*, 2016, **55**, 15250–15253.
- 43 6 M. M. Ali, M. Wolfe, K. Tram, J. Gu, C. D. M. Filipe, Y. Li and J. D. Brennan,  
44 *Angew. Chemie Int. Ed.*, 2019, **58**, 9907–9911.
- 45 7 M. N. Costa, B. Veigas, J. M. Jacob, D. S. Santos, J. Gomes, P. V Baptista, R.  
46 Martins, J. Inácio and E. Fortunato, *Nanotechnology*, 2014, **25**, 094006.
- 47 8 J. Jaeger, F. Groher, J. Stamm, D. Spiehl, J. Braun, E. Dörsam and B. Suess,  
48 *Biosensors*, 2019, **9**, 7.
- 49 9 A. M. Caliendo, D. N. Gilbert, C. C. Ginocchio, K. E. Hanson, L. May, T. C. Quinn,  
50 F. C. Tenover, D. Alland, A. J. Blaschke, R. A. Bonomo, K. C. Carroll, M. J.  
51  
52  
53  
54  
55  
56  
57  
58  
59  
60

- 1  
2  
3 Ferraro, L. R. Hirschhorn, W. P. Joseph, T. Karchmer, A. T. MacIntyre, L. B.  
4 Reller and A. F. Jackson, *Clin. Infect. Dis.*, 2013, **57**, S139–S170.  
5  
6 10 S. Nayak, N. R. Blumenfeld, T. Laksanasopin and S. K. Sia, *Anal. Chem.*, 2017,  
7 **89**, 102–123.  
8  
9 11 K. Pardee, A. A. Green, M. K. Takahashi, D. Braff, G. Lambert, J. W. Lee, T.  
10 Ferrante, D. Ma, N. Donghia, M. Fan, N. M. Daringer, I. Bosch, D. M. Dudley, D.  
11 H. O'Connor, L. Gehrke and J. J. Collins, *Cell*, 2016, **165**, 1255–1266.  
12  
13 12 Y. Ma, G. Mao, Y. Zhong, G. Wu, W. Wu, Y. Zhan, Z. He and W. Huang, *Talanta*,  
14 2019, **194**, 199–204.  
15  
16 13 K. Pardee, A. A. Green, T. Ferrante, D. E. Cameron, A. DaleyKeyser, P. Yin and  
17 J. J. Collins, *Cell*, 2014, **159**, 940–54.  
18  
19 14 C. Tuerk, L. Gold, *Science*, **249**, 505–510.  
20  
21 15 A. D. Ellington, J. W. Szostak, *Nature*, **346**, 818–822.  
22  
23 16 P. Kalra, A. Dhiman, W. C. Cho, J. G. Bruno and T. K. Sharma, *Front. Mol.*  
24 *Biosci.*, 2018, **5**, 41.  
25  
26 17 Q. Zhu, G. Liu, M. Kai and A. O. A. Miller, *Molecules*, 2015, **20**, 20979–90997.  
27  
28 18 G. S. Filonov, J. D. Moon, N. Svensen and S. R. Jaffrey, *J. Am. Chem. Soc.*,  
29 2014, **136**, 16299–16308.  
30  
31 19 M. You and S. R. Jaffrey, *Annu. Rev. Biophys.*, 2015, **44**, 187–206.  
32  
33 20 J. S. Paige, T. Nguyen-Duc, W. Song and S. R. Jaffrey, *Science.*, 2012, **335**,  
34 1194.  
35  
36 21 J. S. Paige, K. Y. Wu and S. R. Jaffrey, *Science*, 2011, **333**, 642–646.  
37  
38 22 M. You, J. L. Litke and S. R. Jaffrey, *Proc. Natl. Acad. Sci.*, 2015, **112**, 2756–  
39 2765.  
40  
41 23 A. P. K. K. Karunanayake Mudiyansele, Q. Yu, M. A. Leon-Duque, B. Zhao, R.  
42 Wu and M. You, *J. Am. Chem. Soc.*, 2018, **140**, 8739–8745.  
43  
44 24 M. You, J. L. Litke, R. Wu and S. R. Jaffrey, *Cell Chem. Biol.*, 2019, **26**, 471–481.  
45  
46 25 Q. Yu, J. Shi, A. P. K. K. Mudiyansele, R. Wu, B. Zhao, M. Zhou and M. You,  
47 *Chem. Commun.*, 2019, **55**, 707–710.  
48  
49 26 R. Wu, A. P. K. K. Karunanayake Mudiyansele, F. Shafiei, B. Zhao, Y. Bagheri,  
50 Q. Yu, K. McAuliffe, K. Ren and M. You, *Angew. Chemie Int. Ed.*, 2019, **58**,  
51 18271–18275.  
52  
53 27 K. Ren, R. Wu, A. P. K. K. Karunanayake Mudiyansele, Q. Yu, B. Zhao, Y. Xie,  
54 Y. Bagheri, Q. Tian and M. You, *J. Am. Chem. Soc.*, 2020, **9**, 11748.  
55  
56 28 R. Wu, A. P. K. K. Karunanayake Mudiyansele, K. Ren, Z. Sun, Q. Tian, B.  
57 Zhao, Y. Bagheri, D. Lutati, P. Keshri and M. You, *ACS Appl. Bio Mater.*, 2020,  
58 acsabm.9b01237.  
59  
60 29 C. A. Kellenberger, S. C. Wilson, J. Sales-Lee and M. C. Hammond, *J. Am.*  
*Chem. Soc.*, 2013, **135**, 4906–4909.  
30  
31 W. A. Haseltine and R. Block, *Proc. Natl. Acad. Sci. U. S. A.*, 1973, **70**, 1564–

- 1  
2  
3 1568.  
4  
5 31 K. Pardee, A. A. Green, T. Ferrante, D. E. Cameron, A. DaleyKeyser, P. Yin and  
6 J. J. Collins, *Cell*, 2014, **159**, 940–954.  
7  
8 32 M. Zweckstetter, G. Hummer and A. Bax, *Biophys. J.*, 2004, **86**, 3444–3460.  
9  
10 33 I. Chopra and M. Roberts, *Microbiol. Mol. Biol. Rev.*, 2001, **65**, 232–260.  
11  
12 34 C. Manyi-Loh, S. Mamphweli, E. Meyer and A. Okoh, *Molecules*, 2018, **23**, 795.  
13  
14 35 D. Kalia, G. Merey, S. Nakayama, Y. Zheng, J. Zhou, Y. Luo, M. Guo, B. T.  
15 Roembke and H. O. Sintim, *Chem. Soc. Rev.*, 2013, **42**, 305–341.  
16  
17 36 V. Haurlyuk, G. C. Atkinson, K. S. Murakami, T. Tenson and K. Gerdes, *Nat. Rev.*  
18 *Microbiol.*, 2015, **13**, 298–309.  
19  
20 37 M. E. Sherlock, N. Sudarsan and R. R. Breaker, *Proc. Natl. Acad. Sci. U. S. A.*,  
21 2018, **115**, 6052–6057.  
22  
23  
24  
25  
26  
27  
28  
29  
30  
31  
32  
33  
34  
35  
36  
37  
38  
39  
40  
41  
42  
43  
44  
45  
46  
47  
48  
49  
50  
51  
52  
53  
54  
55  
56  
57  
58  
59  
60

## Figure Legends

**Figure 1.** Performance of Broccoli in the paper substrate. (a) Effect of BSA concentration on the Broccoli fluorescence. (b) Kinetics of Broccoli fluorescence activation in the paper. The representative images of paper-based Broccoli fluorescence after 0, 5, 10, 15, 20, and 30 min incubation with 1  $\mu\text{M}$  of Broccoli RNA (8 pmol) were shown. Scale bar, 2.5 mm. (c) Detection range of Broccoli RNA in the presence of 20  $\mu\text{M}$  (0.16 nmol) DFHBI-1T in either freshly prepared (0 h) or freeze-dried (48 h) paper substrate. (d) Stability of Broccoli in the freeze-dried paper substrate. Fluorescence signal was measured after different days of storage at room temperature. Shown are mean and SD values of three independent replicates.

**Figure 2.** Paper-based Broccoli tetracycline sensor. (a) Schematic of tetracycline-induced structural change in the sensor and fluorescence activation. The sensor platform comprises an F30 scaffold (black) and a Broccoli-based tetracycline sensor. Tetracycline binding to the aptamer (blue) stabilizes the transducer duplex (gray dashed line), enabling Broccoli (green) to fold and activate the fluorescence of DFHBI-1T. (b) Dose-response curve for the fluorescence detection of tetracycline in buffer and river water sample. The representative images of paper-based sensor fluorescence (top row, buffer; bottom row, surface water) at tetracycline concentrations of 10, 40, 100, 500, 750, and 1000  $\mu\text{M}$  after 30 min incubation were shown. (c) Kinetics of tetracycline (TC)-induced fluorescence activation in the paper substrate. The representative images of paper-based sensor fluorescence at 15, 20, 25, and 30 min after adding 750  $\mu\text{M}$  tetracycline were shown. Shown are mean and SD values of three independent replicates. Scale bar, 2.5 mm.

**Figure 3.** Performance of Broccoli-based tetracycline sensor. (a) Selectivity of the tetracycline sensor as measured in the presence of 1  $\mu\text{M}$  sensor RNA, 10  $\mu\text{M}$  DFHBI-1T, and 750  $\mu\text{M}$  of each antibiotic. The representative images of paper-based sensor fluorescence 30 min after adding each antibiotic were shown. (b) Stability of the tetracycline sensor as measured after different days of storage at room temperature. The representative images of paper-based sensor fluorescence at each time point after adding 1 mM tetracycline were shown. Shown are mean and SD values of three independent replicates. Scale bar, 2.5 mm.

**Figure 4.** Paper-based Broccoli ppGpp sensor. (a) Schematic of ppGpp-induced structural change in the sensor and fluorescence activation. (b) Dose-response curve

1  
2  
3 for the fluorescence detection of ppGpp. The representative images of paper-based  
4 sensor fluorescence at each ppGpp concentrations of 0.05, 0.1, 0.5, 1, 5, 10, and 50  $\mu\text{M}$   
5 after 30 min incubation were shown. (c) Kinetics of ppGpp-induced fluorescence  
6 activation in the paper substrate. The representative images of paper-based sensor  
7 fluorescence at 0, 5, 10, 15, 20, and 30 min after adding 50  $\mu\text{M}$  ppGpp were shown. (d)  
8 Detection range of ppGpp sensor in either freshly prepared (0 h) or freeze-dried (48  
9 h) paper substrate. Shown are mean and SD values of three independent replicates.  
10 Scale bar, 2.5 mm.  
11  
12  
13  
14  
15

16 **Figure 5.** Performance of Broccoli-based ppGpp sensor. (a) Selectivity of the ppGpp  
17 sensor as measured in the presence of 1  $\mu\text{M}$  sensor RNA, 10  $\mu\text{M}$  DFHBI-1T, and 10  $\mu\text{M}$   
18 of each indicated compound. The representative images of paper-based sensor  
19 fluorescence 30 min after adding each compound were shown. (b) Performance of  
20 ppGpp sensor in the presence of *E. coli* cell lysate and 1  $\mu\text{M}$  ppGpp. The  
21 representative images of corresponding paper-based sensor fluorescence were shown.  
22 Shown are mean and SD values of three independent replicates. Scale bar, 2.5 mm.  
23  
24  
25  
26  
27  
28  
29  
30  
31  
32  
33  
34  
35  
36  
37  
38  
39  
40  
41  
42  
43  
44  
45  
46  
47  
48  
49  
50  
51  
52  
53  
54  
55  
56  
57  
58  
59  
60

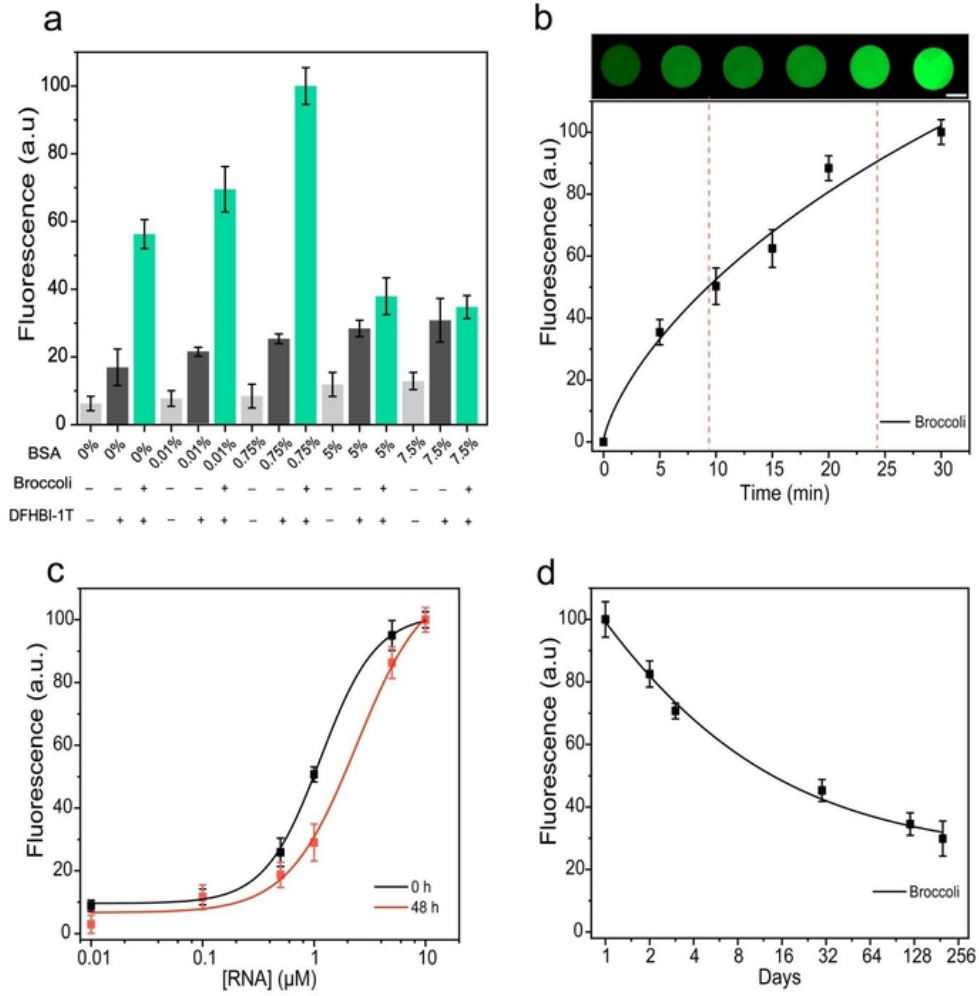


Figure 1

59x60mm (300 x 300 DPI)

1  
2  
3  
4  
5  
6  
7  
8  
9  
10  
11  
12  
13  
14  
15  
16  
17  
18  
19  
20  
21  
22  
23  
24  
25  
26  
27  
28  
29  
30  
31  
32  
33  
34  
35  
36  
37  
38  
39  
40  
41  
42  
43  
44  
45  
46  
47  
48  
49  
50  
51  
52  
53  
54  
55  
56  
57  
58  
59  
60

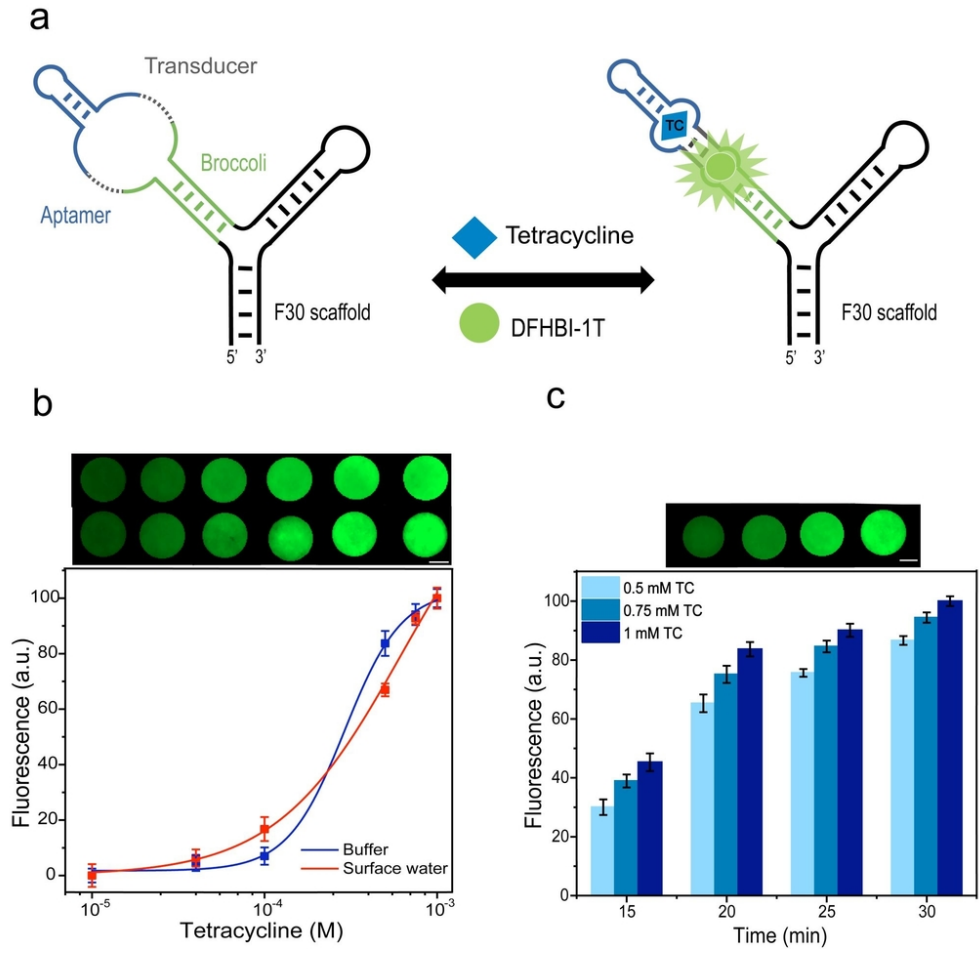


Figure 2

86x82mm (300 x 300 DPI)

1  
2  
3  
4  
5  
6  
7  
8  
9  
10  
11  
12  
13  
14  
15  
16  
17  
18  
19  
20  
21  
22  
23  
24  
25  
26  
27  
28  
29  
30  
31  
32  
33  
34  
35  
36  
37  
38  
39  
40  
41  
42  
43  
44  
45  
46  
47  
48  
49  
50  
51  
52  
53  
54  
55  
56  
57  
58  
59  
60

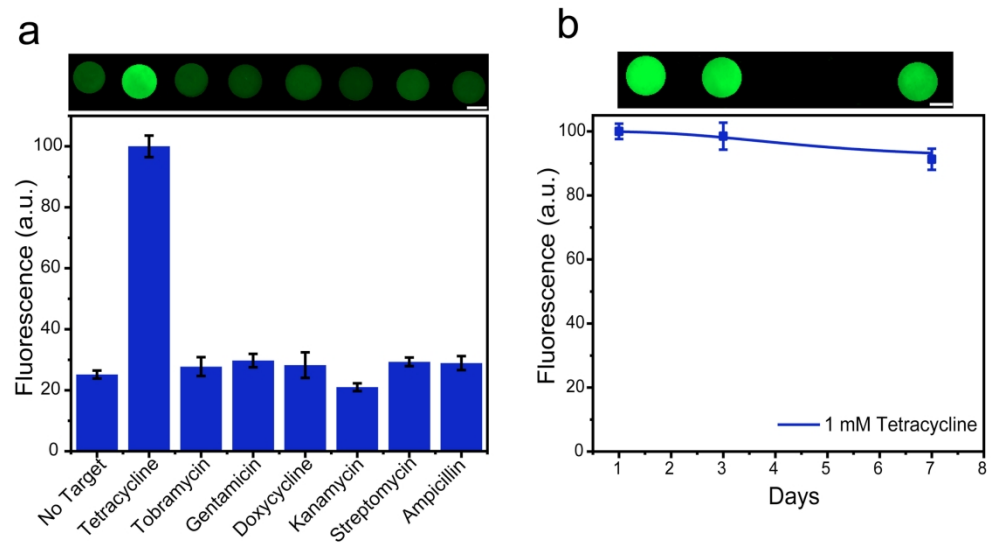


Figure 3

254x138mm (300 x 300 DPI)

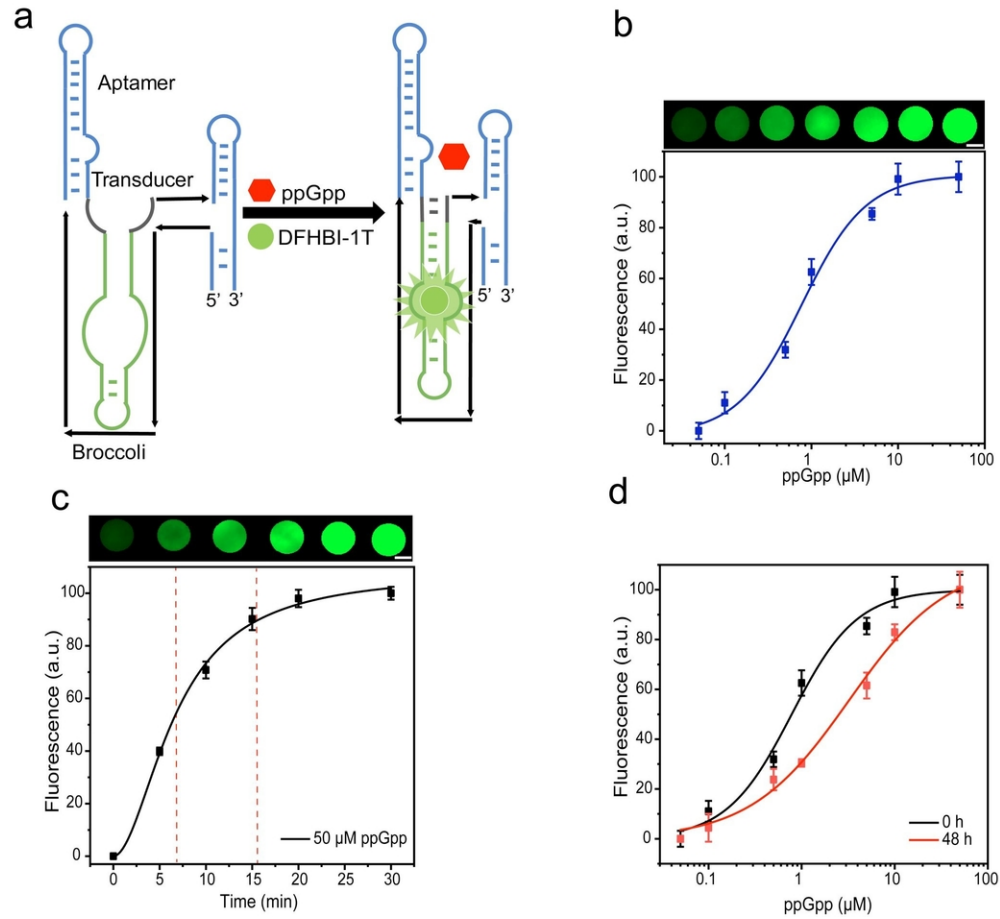


Figure 4

88x81mm (300 x 300 DPI)

1  
2  
3  
4  
5  
6  
7  
8  
9  
10  
11  
12  
13  
14  
15  
16  
17  
18  
19  
20  
21  
22  
23  
24  
25  
26  
27  
28  
29  
30  
31  
32  
33  
34  
35  
36  
37  
38  
39  
40  
41  
42  
43  
44  
45  
46  
47  
48  
49  
50  
51  
52  
53  
54  
55  
56  
57  
58  
59  
60

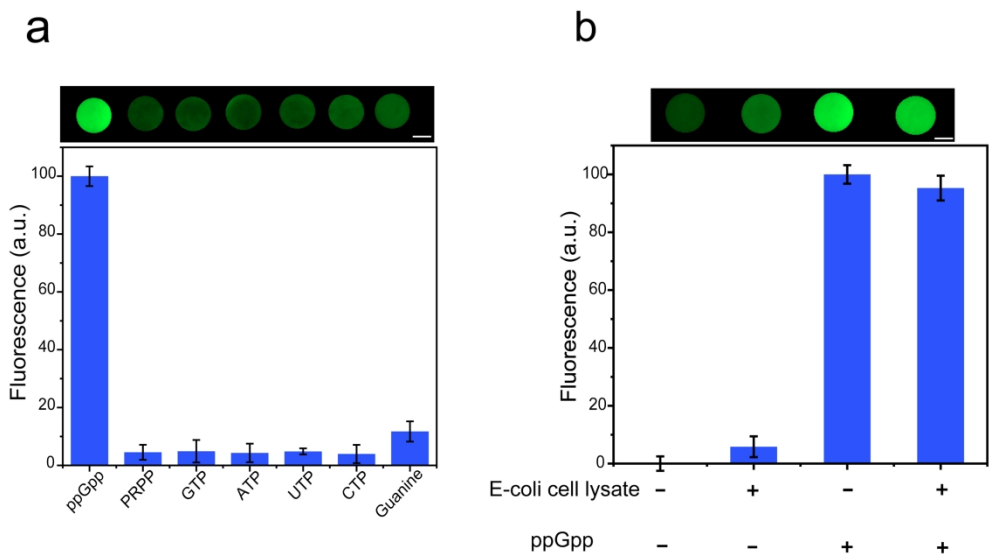
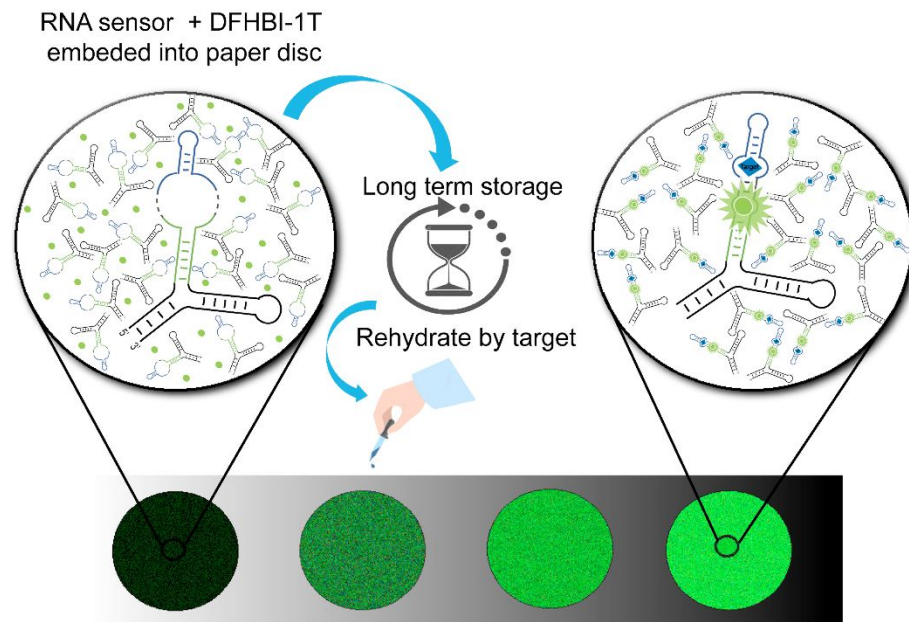


Figure 5

301x168mm (300 x 300 DPI)

## Table of Contents



A paper-based portable fluorogenic RNA sensor for the selective, sensitive, and rapid detection of target analytes.